Appl. Magn. Reson. 29, 1–XXX (2005)

Applied Magnetic Resonance

Diffusion and Aggregation of Alzheimer's $A\beta_{1\text{-}40}$ Peptide in Aqueous-TFE Solutions as Studied by Pulsed Field Gradient NMR

A. Filippov[1,2], **A. Sulejmanova**[2], **O. Antzutkin**[3], and **G. Gröbner**[1]

[1] Umeå University, Umeå, Sweden
[2] Kazan State University, Kazan, Russian Federation
[3] Lulea University of Technology, Lulea, Sweden

Received July 1, 2005; revised August 3, 2005

Abstract. Pulsed field gradient nuclear magnetic resonance technique was applied to measure the self-diffusion coefficient of $A\beta_{1\text{-}40}$ peptide in trifluoroethanol (TFE) and mixed solvent TFE–water (D_2O) buffer (pD 7.8) at 293 K. The data were analyzed on the basis of the Stokes model and the hard- sphere approach was used to estimate self-diffusion coefficients. It was found that the extent of the $A\beta_{1\text{-}40}$ aggregation in TFE solutions depends on the concentration of the peptide and the sample preparation protocol. After soft mixing, i.e., without any additional mechanical pretreatment of the peptide, the peptide is present in the monomeric form in TFE solutions. However, the additional water-bath sonication of the sample during the dissolution of $A\beta_{1\text{-}40}$ in TFE enforces oligomerization of the peptide with the size of aggregates ranging from tetra- to hexamers. An increase of D_2O in the mixed TFE–D_2O solvent of up to 75% leads to the aggregation of the large part of the peptide. However, the components of self-diffusion coefficients related to low-mass $A\beta_{1\text{-}40}$ oligomers (dimers and trimers) were not observed in the diffusion decay curves. The most probable explanation is that dimers and trimers are not the principal intermediate species in the aggregation of $A\beta_{1\text{-}40}$ peptide.

1 Introduction

Alzheimer's disease (AD) is a chronic dementia, affecting an increasing part of the human population [1–3]. Along with the mature onset diabetes and prion-transmissible spongiform encephalopathies, AD belongs to a category of amyloid diseases, which are all categorized by an abnormal folding of normally soluble peptides into neurotoxic aggregated structures [3–5]. The key event in AD is the metabolism of the amyloid precursor protein to the amyloid-β (Aβ) peptide and the subsequent deposition of aqueous Aβ-containing aggregates as amyloid plaques or fibrils in the brains of patients [3–5]. This 39-42 amino acid peptide has been linked to the apoptosis of neuronal cells, and its neurotoxicity seems to be closely related to the pathological conversion or "misfolding" from the normal nontoxic globular or "natively unfolded" structure into toxic aggre-

gates, a process not yet understood, despite recent progress [3–6]. An important feature seems to be that Aβ peptide is released as a monomeric soluble peptide, but requires a minimal level of aggregation to exert its neurotoxic action [3–8]. Due to the complexity and dependence of this process on physiological parameters, various models for fibril formation are discussed. Structural and biophysical studies of the self-assembly of Aβ peptide into fibrillar structures found this process strongly dependent on the physical conditions [3–8]. While earlier studies proposed antiparallel-β-sheet structures for the amyloid fibrils, more recent work indicates an in-register, parallel organization of β-sheets propagating and twisting along the fibrillar axis [9]. However, there is growing evidence that the toxic agent is not the mature fibrils themselves, but oligomeric and protofibrillar Aβ-structures which can be associated with the neuropathological events causing the deterious conditions of AD patients [4, 8]. Recently, the discovery of various soluble amyloid oligomers having a common structure, independently of their location in extracellular or intracellular compartments, brought new insight into possible mechanisms of toxicity. However, there is still no common view how globular and nonfibrillar Aβ which is continuously released during normal metabolism, can exert its cytotoxic action by forming toxic aggregates.

One approach to obtain insight into this process is the study of Aβ peptide in water solution, where it was shown to associate into oligomeric aggregates [3, 4]. Here we study the first steps of the peptide aggregation in bulk solution, as a model for its in vivo aggregation process (preaggregation) in tissues. This preaggregation phenomenon can usually be proposed as oligomer formation including a small number of peptides as the first and important step of fibril formation. Since these early events are not studied in detail, we used nuclear magnetic resonance with pulsed field gradient (PFG NMR) which is sensitive to the aggregation process and to the size of aggregates. The method can provide direct and rather simple relation of the molecule (aggregate) molecular mass and the corresponding diffusion coefficient [10–16]. For example, Gräslund and coworkers [11, 12] investigated the $A\beta_{12-28}$ fragment in water solutions and found that the peptide exists in the monomeric, random coil conformation. Tseng and coworkers [17] also showed that the peptide is mostly monomeric. Hou and coworkers [18] demonstrated that the peptide is predominantly monomeric at neutral pH. Narayanan and Reif [19] studied diffusion of $A\beta_{1-40}$ in water solutions with varying NaCl concentrations and obtained the peptide diffusion coefficient corresponding (with a spherical Stokes model) to the molecular weight of 20.8 kDa. They concluded that $A\beta_{1-40}$ exists in equilibrium with higher oligomeric state structures and that the peptide appears to adopt on average a tetrameric oligomeric state. In this report, we present the aggregation behavior of Aβ in membrane mimicking TFE and water, where we found a variable specific aggregation pattern during the initial state of the aggregation process.

2 Theory

The diffusion coefficient D of a protein in solution can be calculated with the Stokes–Einstein hydrodynamic equation for a hard sphere moving in a viscous liquid

$$D = \frac{kT}{f} = \frac{kT}{6\eta\pi R},$$

where k is the Boltzmann constant, T is temperature, f is the translational friction coefficient, η is viscosity of the solvent, R is the sphere hydrodynamic radius. With the hard-sphere approximation, D of a particle with a mass M in solution can be described by the following equation [20]

$$D = \frac{Tk}{6\pi\eta}\sqrt[3]{\frac{4\pi N_{\mathrm{A}}\rho_{\mathrm{prot}}}{3M(V2 + \delta_1 V1)}}, \tag{1}$$

where ρ_{prot} is the particle density, N_A is the Avogadro constant, $V1$ is the particle specific volume, $V2$ is the partial specific volume of the solvent, δ_1 is the fractional amount of solvent bound to the particle. Clearly, calculation of M from D requires the values for η, ν_2, and δ_1 to be known.

3 Experimental Part

3.1 Materials and Samples Preparation

Amyloid-$\beta_{1\text{-}40}$ peptide (DAEFRHDSGYEVHHQKLVFFAEDVGSNKGAIIGLMV× GGVV) wild type $M_w = 4331$ was synthesized by standard solid-phase FMOC (peptide synthesis with a conductivity monitoring unit utilizing 9-fluorenylmethoxycarbonyl amino acid derivatives) chemistry, subsequently purified by high performance liquid chromatography and found to be over 90% pure by MALDI-TOF (matrix-assisted laser desorption–ionization mass spectrometry) mass spectroscopy. TFE (trifluoroethanol-d_3) from Larodan Fine Chemicals AB with deuteration level 99% was used. At 293 K is has a density of 1373 kg/m^3 and viscosity of $1.35 \cdot 10^{-3}$ Pa·s. D_2O from Larodan Fine Chemicals AB: density 1110 kg/m^3, viscosity $1.24 \cdot 10^{-3}$ Pa·s was used. Peptide was stored in a refrigerator at -55 °C. For preparation of the TFE solution the required amount of the peptide and TFE were mixed. Measurements were started after 15 min of mixing. Additionally protonated TFE was also measured for comparison and identification of the TFE signal in solution. For the studies with water the D_2O buffer (10 mM TRIS, 10 mM KCl, 0.5 mM EDTA, pD 7.8) was used.

3.2 PFG NMR Technique

Most of diffusion measurements were performed on a Varian/Chemagnetics CMX Infinity spectrometer at 100 MHz for ^{1}H, equipped with a PFG probe (Cryomagnet systems, Indianapolis, IN). The standard stimulated echo pulse sequence was applied. The value of the PFG was set constant (g = 1.15 T/m), and the duration of the pulse δ was varied in 10 to 32 steps while all other variables were held constant. The signal was accumulated for 16 to 320 scans, Fourier-transformed into spectra. These were integrated and fitted into decays to obtain the diffusion constant D. Additional experiments were performed on a homebuilt NMR spectrometer operating at ^{1}H NMR 300 MHz (Kazan, Russian Federation). Diffusion decays were obtained as dependences of the spin-echo amplitude on the pulsed magnetic field amplitude, which was varied stepwise from 0 to the maximum value of 5 T/m. Additional experiments showed the independence of the diffusion coefficient of the diffusion time, which was varied between 60 and 100 ms.

For the stimulated echo pulse sequence used the diffusion decay of the echo amplitude A can be described by the relation [21]

$$A = \frac{I}{2}\exp\left(-\frac{2\tau}{T_2}\right)\exp\left(\frac{\tau_1}{T_1}\right)\exp\left(-\gamma^2\delta^2 g^2 D\left(\Delta - \frac{\delta}{3}\right)\right),$$

where the initial echo amplitude (without the magnetic field gradient) is determined by the longitudinal and transverse NMR relaxation times (T_1 and T_2) and I is a factor proportional to the proton content in the system, γ is the gyromagnetic ratio, Δ is the time interval between the two gradient pulses, $t_d = (\Delta - \delta/3)$ is the diffusion time, and D is the self-diffusion coefficient. All measurements were performed at 293 K.

4 Results

The typical diffusion decay curves obtained by the PFG NMR technique for TFE–buffer mixture are presented in Fig. 1. The diffusion decay for buffer (circles) is nonexponential due to the presence of several types of molecules, HOD and other buffer components. However, the main reason of the nonexponentiality is the difference in the diffusion behavior of HOD and TFE molecules (Fig. 1, dashed and solid lines, respectively). The populations determined for both diffusion components are close to the theoretical ratio of HOD and TFE components in the mixture. However, the values of diffusion coefficients are slightly different compared to the ones obtained in neat liquids of each component, due to the additional solution interactions as known for liquid mixtures. The mean diffusion coefficient is given by

$$D = \sum_i P_i D_i ,$$

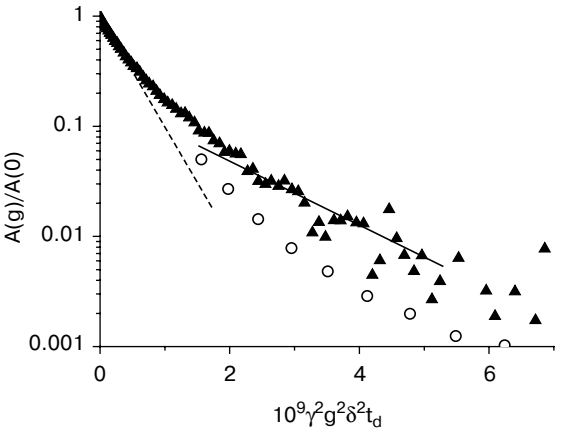

Fig. 1. 300 MHz ^{1}H NMR diffusion decays of D_2O buffer pH 2.0 (TRIS HCl) (circles), and of a mixture TFE–D_2O buffer pH 2 with about 20 wt% of TFE (triangles). Dashed and solid lines correspond to HOD traces in D_2O ($2 \cdot 10^{-9}$ m^2/s) and the TFE ($6.7 \cdot 10^{-10}$ m^2/s) diffusion, respectively.

where P_i and D_i are the fractions and the partial diffusion coefficients, respectively. Taking into account that for a single unique diffusion coefficient of $A\beta_{1\text{-}40}$ monomers as calculated according to Eq. (1), the diffusion decay has a smaller slope than that for the components of the solvent, one can reliably separate the NMR signal risen from protons in $Ab_{1\text{-}40}$ peptide from all other components in the NMR experiment. The diffusion coefficients of pure and mixed solvents are much larger than the diffusion coefficient of the peptide, so the latter can reliably be measured even under the condition of a severe line broadening. In principle, the analysis can be performed without the standard procedure of Fourier transform, i.e., by analyzing the shape of the echo decay.

4.1 Self-Diffusion of $A\beta_{1\text{-}40}$ Peptide in TFE Solution

Two different solutions have been prepared. In the first preparation of $A\beta_{1\text{-}40}$ peptide (soft mixing) the peptide powder was suspended in TFE without any additional mechanical pretreatment. In the second preparation (sonication), the sample tube was sonicated in a water bath for 15 min upon mixing the peptide with TFE solvent. In both cases NMR measurements were started immediately after the sample preparation. In both cases, with and without sonication of the solution peptide, solutions were transparent and no changes in the turbidity could be observed during several days at room temperature.

Figure 2 shows the NMR diffusion decay curves for the sample of $A\beta_{1\text{-}40}$ solution in TFE prepared without sonication. The decay can be described as a sum of two exponentials with the diffusion coefficients $D_{sol} \sim 2 \cdot 10^{-9}$ m^2/s and $D_1 = (1.35 \pm 0.1) \cdot 10^{-10}$ m^2/s, where D_{sol} and D_1 are diffusion coefficients of the solvent molecules and monomers of $A\beta_{1\text{-}40}$ peptide, respectively. This decay curve

was reproducible during several days from the sample preparation up to the end of the experiment.

Fully deuterated TFE molecules do not contain protons in $-$OD and $-CD_2$ groups. However OD^- can exchange OH^- in $A\beta_{1\text{-}40}$ peptide and in water molecules associated with peptide after lyophilization. $A\beta_{1\text{-}40}$ contains a number of amino acid residues with exchangeable protons in hydroxyl groups with a portion of about 22%. Because the solvent is in excess, all the exchangeable protons will have access to TFE solvent. Surprisingly, at 20 °C the value of D_{sol} in the decay (Fig. 2, dashed line) does not correspond to the diffusion coefficient of TFE ($6.7 \cdot 10^{-10}$ m^2/s), but is closer to D of water (about $2 \cdot 10^{-9}$ m^2/c). An explanation might be the presence of adsorbed (bound) water in initially dry lyophilized peptide powder in quantities comparable with exchangeable protons of TFE (1 of 3, i.e., 33%). The real populations of diffusion components in Fig. 2 are different from the estimated ratios of protons of the peptide in TFE and $A\beta_{1\text{-}40}$ peptide. These are conditioned by the accelerated transverse NMR relaxation of protons of the peptide as well as by the presence of water molecules, which were not taken into account.

The diffusion coefficient of monomers of $A\beta_{1\text{-}40}$ peptide was calculated together with the hydrodynamic radius for $A\beta_{1\text{-}40}$ with Eq. (1) and further compared with D_1 obtained from the ^{1}H NMR diffusion decay (Fig. 2). The values taken in these calculations were $T = 293$ K and $\eta_{TFE} = 1.75 \cdot 10^{-3}$ mPa$\cdot$s [16]. The estimated values of the hydrodynamic radius R and the diffusion coefficient of $A\beta_{1\text{-}40}$ monomers are $1.1 \cdot 10^{-9}$ m and $1.42 \cdot 10^{-10}$ m^2/s, respectively. This calculated value for D is quite close to the experimentally obtained value in our experiment $(1.35 \pm 0.1) \cdot 10^{-10}$ m^2/s. Thus, these results clearly indicate that

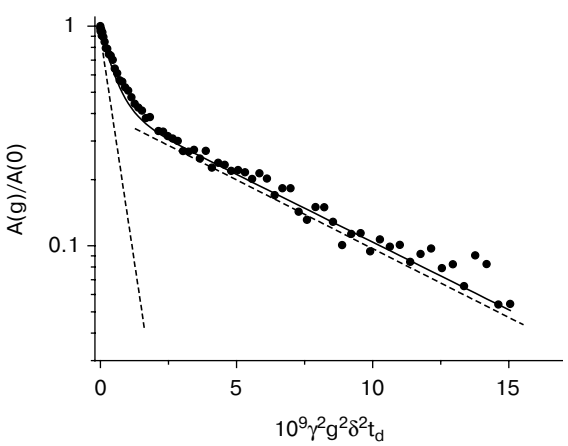

Fig. 2. 300 MHz ^{1}H NMR diffusion decay of $A\beta_{1\text{-}40}$ peptide in TFE solution (3 mM/l, 0.99 wt%) prepared by soft mixing (without sonication). The measurement parameters are $\delta = 0.36$ ms, $t = 2.5$ ms, $t_d = 61$ ms, and $g = 0$–5 T/m. Dashed lines, slopes corresponding to $D_{sol} \sim 2 \cdot 10^{-9}$ m^2/s (solvent diffusion coefficient) and $D_1 \sim 1.35 \cdot 10^{-10}$ m^2/s (the diffusion coefficient of $A\beta_{1\text{-}40}$ monomers). Solid line, sum of the two components.

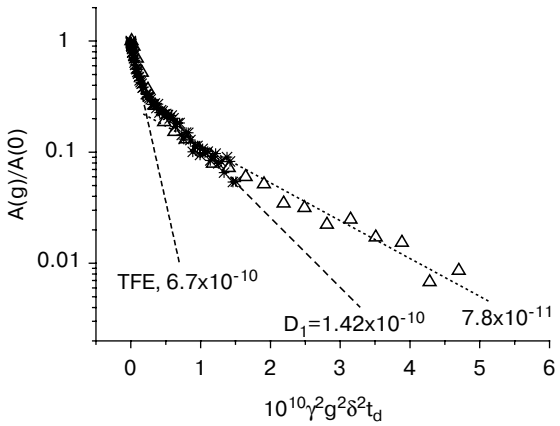

Fig. 3. 100 MHz ^{1}H NMR diffusion decay in the sonicated sample of $A\beta_{1-40}$ peptide of TFE solution (69 μM/l) (triangles). The measurement parameters are $g = 1.5$ T/m, $t = 4$ ms, $t_d = 100$ ms, and $\delta = 0.1$–3 ms. Dashed lines, $D = 1.42 \cdot 10^{-10}$ m^2/s ($A\beta_{1-40}$ monomers) and $D_{sol} = 6.7 \cdot 10^{-10}$ m^2/s (TFE). Dotted line, $D = 7.8 \cdot 10^{-10}$ m^2/s, which is close to the calculated diffusion coefficient of $A\beta_{1-40}$ hexamers. Stars, data points are taken from Fig. 2.

for the case of soft mixing of $A\beta_{1-40}$ peptide in TFE, the peptide is present in the solution in the monomeric form and can be described by the model of a hard sphere with a radius R. In addition, the lyophilized peptide contains some adsorbed water, which governs the mean diffusion coefficient of the component in the ^{1}H NMR diffusion decay of solvent molecules.

Figure 3 presents the diffusion decay curves for another sample of $A\beta_{1-40}$ in TFE prepared under sonication for 15 min prior to the experiments. Here, the decay has a similar form as in the case of soft mixing (stars). However, D_{sol} now is about $6.7 \cdot 10^{-10}$ m^2/s, which is equal to the TFE diffusion coefficient. No water diffusion coefficient (originating from adsorbed water) was observed because a lower peptide concentration was used. This decrease of the diffusion coefficient cannot be related to concentration effects, because a decrease in concentration would be accompanied with a simultaneous decrease of probability of interparticle collisions. For the peptide diffusion coefficient one can already see the difference from the monomeric diffusion coefficient (dashed line). The observed diffusion coefficient is $7.8 \cdot 10^{-11}$ m^2/s. According to Eq. (1), it corresponds to aggregates with the sizes, which can be estimated in the simplest case of a spherical form as hexamers. The observed decay was not changing during the whole time of study (up to 48 h), so, no further aggregation and no disaggregation processes were observed.

Thus, the $A\beta_{1-40}$ peptide aggregation structure in TFE solution depends on the solution preparation. In the case of soft treatment, a monomeric form exists, but sonication leads to the formation of higher oligomers, which are close to hexamers in average. In our other experiments of this type (with sonication) we observed diffusion coefficients corresponding to tetramers, hexamers and higher than hexamers, no dimers were observed.

4.2 Self-Diffusion in TFE–Water Mixtures

In the next step of our experiments with the TFE solution, which showed monomeric $Ab_{1\text{-}40}$ diffusion coefficient (Fig. 2), we added the water (D_2O) buffer (pD 7.0) stepwise up to obtaining concentration of mixed solution which we desired. Measurements were performed at 47, and 25 wt% of TFE.

The solution at the concentration of 47 wt% of TFE remained transparent. Diffusion decay for it is shown in Fig. 4 (open circles). Populations of the decay components remain unchanged in comparison with TFE solution. However, the diffusion coefficient of peptide is smaller, $D \sim (1.21 \pm 0.11) \cdot 10^{-10}$ m^2/s. This effect cannot be related with oligomerization, because even for dimers the diffusion coefficient will be much smaller, about $D_2 = 8.9 \cdot 10^{-11}$ m^2/s. The next probable explanation lies in the dependence of hydrodynamic parameters of the mixed solvent on the water concentration. In fact, the viscosity of TFE–water showed an extreme dependence with a maximum at about 50 wt%. According to Shuck et al. [22], this dependence is described at 20 °C by

$$\eta = 1.000 + 2.133x + 1.670x^2 - 8.404x^3 + 4.948x^4 . \qquad (2)$$

We used the correction for viscosity in the calculation of the monomeric diffusion coefficient in TFE–water and obtained the value $D_1 = 1.12 \cdot 10^{-10}$ m^2/s (showed as dashed line), which was really measured in this mixed solvent for the less mobile molecules. So, it is evident that the change of the solvent viscosity described the observed change of the peptide monomer diffusion coefficient. No dimerization and no conformation changes are needed to describe this experimental effect.

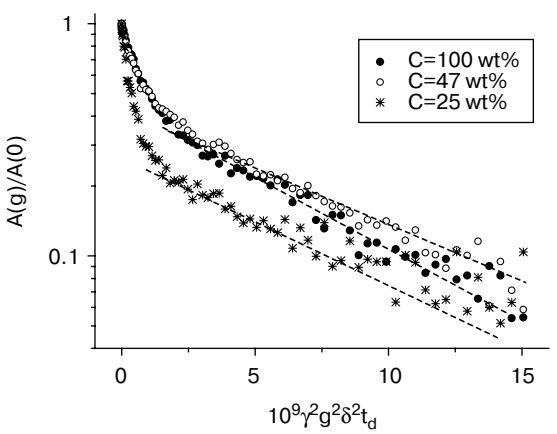

Fig. 4. Diffusion decay in solutions of $A\beta_{1\text{-}40}$ peptide in mixed solvent TFE–D_2O at indicated concentrations C of TFE and pD 7.0 of D_2O. Peptide concentration for $C = 100$ wt% was 3 mM/l, for $C = 47$ wt% was 1.5 mM/l, and for $C = 25$ wt% was 0.83 mM/l. Dashed lines correspond to calculated monomer diffusion at different concentrations of TFE ($1.42 \cdot 10^{-10}$ m^2/s for 100 wt%, $1.12 \cdot 10^{-10}$ m^2/s for 47 wt%, and $D_1 \sim 1.28 \cdot 10^{-10}$ m^2/s for 25 wt% of TFE).

Further increase of the water content was up to 75 wt% of water buffer and 25 wt% of TFE. The solution became turbid. Diffusion decay (stars in Fig. 4) showed the decrease of the population for the peptide component, whereas the diffusion coefficient for this component increased up to $D = (1.31 \pm 0.1) \cdot 10^{-10}$ m^2/s. The correction in viscosity according to Eq. (2), gives $\eta = 1.53 \cdot 10^{-3}$ $Pa \cdot s$ and leads to $D_1 = 1.28 \cdot 10^{-10}$ m^2/s for the monomeric diffusion coefficient. So the observed diffusion coefficient for peptide as evident from Fig. 4 (stars and dashed line crossing them) can be again related only to monomer diffusion. The decrease of the population of the peptide signal, which was observed for this concentration, can be due to the increase of T_2 of the peptide protons in the aggregated state (which was observed as a turbid part of the solution). However, the "visible" part of the peptide remains in the monomeric form, so we observed the decreased signal from the peptide but with the monomeric diffusion coefficient.

For the TFE concentration of 10 wt% and less the solution was turbid, no signal from peptide was observed.

Thus, the observed mean value of the diffusion coefficient for peptide in the mixed TFE–water solvent corresponds to the concentration dependence of the monomer diffusion in this mixed solvent. No signal from dimers and higher-mers were observed. The aggregation process resulted in the decrease of populations corresponding to the peptide signal.

5 Discussion

Our results showed that the Stokes model and the hard-sphere approach can be applied to describe monomeric $A\beta_{1\text{-}40}$ peptide diffusion not only in water solutions, but also in TFE and mixed TFE–water solutions. Changes in the solvent viscosity due to their concentration dependence influences the peptide diffusion coefficient and can be taken into account. TFE–water solvent does not influence the structural characteristics essential for the translational mobility of the $A\beta_{1\text{-}40}$ monomer. Sonication of the peptide in the solution of TFE lead to the formation of stable aggregates from tetramer to higher than hexamers according to their hydrodynamic properties. Thus our results coincide with previous ones [11, 17, 19], which showed that PFG NMR technique can be used for the measurement of monomeric diffusion coefficient of $A\beta_{1\text{-}40}$ in solution.

We also did not observe any nonmonomeric forms of the peptide (dimers and higher-mers) in water solutions. A probable explanation was proposed by Jarvet and co-workers [11]. They concluded that the signal from dimers and higher-mers of $A\beta_{1\text{-}40}$ peptide in water solution was not observed because of the accelerated T_2 relaxation in the peptide aggregates. In our opinion, this conclusion seems to hold for small-number oligomeric states. Indeed, we know that $A\beta_{1\text{-}40}$ peptide in water solution is of a globular structure [11, 12]. The main mechanism which leads to the accelerated transverse NMR relaxation of globular proteins is the dipolar interaction. Globular proteins are tightly packed structures with strong dipolar interactions. Averaging of the dipolar interaction is due not

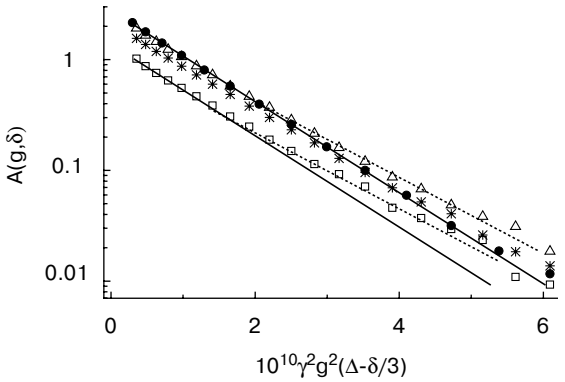

Fig. 5. Diffusion decays of lysozyme in water solution at pH 4.5 in different stages of aggregation at 330 K at time after mixing: 12 (circles), 96 (triangles), 192 (stars) and 528 (squares) h. Solid lines show calculated diffusion coefficient (Eq. (2)) for monomer ($9.24 \cdot 10^{-11}$ m^2/s), whereas dotted lines for dimer ($7.33 \cdot 10^{-11}$ m^2/s) (A. Filippov et al., unpubl.).

to the local segmental motion, but to the fast rotation of the protein molecule as a whole. For small globular proteins, the dipolar Hamiltonian can be averaged effectively only due to the anisotropic rotational diffusion of the molecule as a whole [23]. Therefore, the reason for the signal from aggregates to disappear was the retardation of the rotational mobility of aggregates. In the first set of the experiments, we used sonication of TFE solution which leads to rather small aggregates, which are still "visible" in the NMR diffusion experiments as tetra- or hexamers. In the second set, we added a water buffer at concentrations of about 50 wt% and higher. Disappearance of the signal from oligomers in this case means that aggregates are rather large, without any intermediate sizes like dimers, tetramers and those close to these sizes. Probably this was the reason why in other NMR experiments with aggregation of peptides in water solutions only monomeric forms of Aβ peptide were visible [11, 17]. Only Narayanan and Reif [19] finally observed intermediate oligomeric states of $A\beta_{1\text{-}40}$ peptide upon variation of the anionic strength of the buffer, which is not the case in our study.

In a previous study one of the authors (A. Filippov et al., unpubl.) investigated aggregation of lysozyme (14.6 kDa) in a water buffer and directly observed diffusion of dimers (Fig. 5), showing that dimers are preaggregation entities for aggregation in lysozyme. The absence of the $A\beta_{1\text{-}40}$ dimer signal at the condition of the partial peptide aggregation (Fig. 4, stars) and the size of the $A\beta_{1\text{-}40}$ dimer being much less than the size of the lysozyme dimer mean that dimerization is not a step of aggregation in $A\beta_{1\text{-}40}$ peptide.

Acknowledgments

This work was supported by Knut and Alice Wallenberg Foundation, Swedish Research Council (621-2001-3185), Umeå University Biotechnology Fund, Natural

Science Faculty and Alzheimer Foundation, and Russian Foundation for Basic Research (04-03-32861). L. Johansson, G. Örrad, and G. Lindblom and his group are gratefully acknowledged for all their support.

References

1. Masters C.L., Simms G., Weinman N.A., Multhaup G., McDonald B.L., Beyreuther K.: Proc. Nat. Acad. Sci. USA **82**, 4245–4249 (1985)
2. Haass C., Selkoe D.J.: Cell **75**, 1039–1042 (1993)
3. Iversen L.L., Mortishire-Smith R.J., Pollack S.J., Shearman M.S.: Biochem. J. **311**, 1–16 (1995)
4. Rochet J.-C., Lansbury Jr. P.T.: Curr. Opin. Struct. Biol. **10**, 60–68 (2000)
5. Kosik K.S.: Proc. Nat. Acad. Sci. USA **96**, 2574–2576 (1999)
6. Bucciantini M., Giannoni E., Chiti F., Baroni F., Formigli L., Zurdo J., Taddei N., Ramponi G., Dobson C.M., Stefani M.: Nature **416**, 507–511 (2002)
7. Lansbury Jr. P.T.: Proc. Nat. Acad. Sci. USA **96**, 3342–3344 (1999)
8. Kayed R., Head E., Thompson J.L., McIntire T.M., Milton S.C., Cotman C.W., Glabe C.: Science **300**, 486–489 (2003)
9. Antzutkin O.N., Balbach J.J., Leapman R.D., Rizzo N.W., Reed J., Tycko R.: Proc. Nat. Acad. Sci. USA **97**, 13045–13050 (2000)
10. Lorenzo A., Yuan M., Zhang Z., Paganetti P.A., Sturchler-Pierrat C., Staufenbiel M., Mautino J., Vigo F.S., Sommer B., Yankner B.A.: Nature Neurosci. **3**, 460–464 (2000)
11. Jarvet J., Damberg P., Bodell K., Eriksson L.E.G., Gräslund A.: J. Am. Chem. Soc. **122**, 4261–4268 (2000)
12. Danielsson J., Jarvet J., Damberg P., Gräslund A.: Magn. Reson. Chem. **40**, S89–S97 (2002)
13. Price W.S., Tsuchiya F., Arata Y.: J. Am. Chem. Soc. **121**, 11503–11512 (1999)
14. Jones J.A, Wilkins D.K., Smith L.J., Dobson C.M.: J. Biomol. NMR **10**, 199–203 (1997)
15. Wilkins D.K., Grimshaw S.B., Receveur V., Dobson C.M., Jones J.A., Smith L.J.: Biochemistry **38**, 16424–16431 (1999)
16. Yao S., Howlett G.H., Norton R.S.: J. Biomol. NMR **16**, 109–119 (2000)
17. Tseng B.P., Ester W.P., Clish C.B., Stimson E.R., Ghilardi J.R., Vinters H.V., Mantyh P.W., Lee J.P., Maggio J.E.: Biochemistry **38**, 1424–10431 (1999)
18. Hou L., Shao H., Zhang Y., Li H., Menon N.K., Neuhaus E., Brewer J.M., Byeon I.-J.L., Ray D.G., Vitek M.P., Iwashita T., Makula R.A., Przybyla A.B., Zagorski M.: J. Am. Chem. Soc. **126**, 1992–2005 (2005)
19. Narayanan S., Reif B.: Biochemistry **44**, 1444–1452 (2005)
20. Krishnan V.V.: J. Magn. Reson. **124**, 468–473 (1997)
21. Stejskal E.O., Tanner J.E.: J. Chem. Phys. **42**, 288 (1965)
22. Shuck P., MacPhee C.E., Howlett G.J.: Biophys. J. **74**, 466–474 (1998)
23. Fushman D., Varadan R., Assfalg M., Walker O.: Progr. NMR Spec. **44**, 189–214 (2004)

Authors' address: Gerhard Gröbner, Department of Biophysical Chemistry, Umeå University, SE-90187 Umeå, Sweden
E-mail: Gerhard.Grobner@chem.umu.se